

Finite Element Analysis of Contact Behavior in Thick-Walled Cylinders

Mohamed Elrawemi ^{1*}, Ali Aburass ², Moamar Hamed ³

¹ Department of Mechanical and Industrial Engineering, Faculty of Engineering, Elmergib University, Al-Khums, Libya

² Department of Mechanical Engineering Technologies, Higher Institute of Science and Technology, Zawia, Libya

³ Department of Mechanical and Industrial Engineering, Faculty of Engineering, Alasmarya Islamic University, Zliten, Libya

التحليل بالعناصر المتناهية لسلوك التلامس في الأسطوانات سميك الجدار

محمد الرومي^{1*}، علي أبوراس²، معمر احمد³

¹ قسم الهندسة الميكانيكية والصناعية، كلية الهندسة، جامعة المرقب، الخمس، ليبيا

² قسم تقييمات الهندسة الميكانيكية، المعهد العالي للعلوم والتكنولوجيا، الزاوية، ليبيا

³ قسم الهندسة الميكانيكية والصناعية، كلية الهندسة، الجامعة الأسلامية الإسلامية، زلiten، ليبيا

*Corresponding author: mselrawemi@elmergib.edu.ly

Received: November 16, 2025

Accepted: January 25, 2026

Published: February 08, 2026

Abstract

Shrink-fit assemblies of dissimilar materials, such as aluminum and steel, are widely used in thick-walled structural components to transfer loads without mechanical fasteners. These assemblies offer advantages in weight reduction, compactness, and manufacturing efficiency. However, accurate prediction of stress distribution in such systems remains challenging, as it depends on internal pressure, interference-induced shrinkage pressure, and cylinder geometry. Classical analytical approaches, including Lamé's equations and Hertzian contact theory, are insufficient for accurately predicting contact stresses, plastic deformation, and residual stresses when nonlinear material behavior and large deformations become significant.

In this study, nonlinear finite element analysis using ABAQUS was conducted to investigate the contact pressure, stress distribution, and plastic deformation in two concentric, open-ended aluminum and steel cylinders subjected to shrink-fit conditions. A preload of 66.5 MN/m² was initially applied and subsequently released to achieve a target interference pressure of 1 MN/m² at the interface between the two cylinders. After unloading, half of the original preload (33.25 MN/m²) was reapplied to investigate stress evolution, residual stress development, and material interaction. The obtained results were then compared with those of a single aluminum cylinder subjected to a preload of 66.5 MN/m². The comparison demonstrates that the compound shrink-fit configuration improves stress distribution and reduces peak stresses. These results provide a framework for designing reliable shrink-fit thick-walled assemblies beyond classical methods.

Keywords: Shrink fit, Thick-walled cylinders, Dissimilar materials, Residual stresses, Nonlinear FEA.

الملخص

تُستخدم تجميعات التركيب بالتدخل (Shrink-fit) المصنوعة من مواد غير متماثلة، مثل الألومنيوم والفولاذ، على نطاق واسع في المكونات الإنشائية سميك الجدران لنقل الأحمال دون الحاجة إلى وسائل تثبيت ميكانيكية. وتتوفر هذه الوصلات مزايياً متعددة، من بينها تقليل الوزن، وزيادة التماسك، وكفاءة التصنيع. ومع ذلك، ما تزال عملية التنبؤ الدقيق بتوزيع الإجهادات في هذه الأنظمة تمثل تحدياً، إذ تعتمد على الضغط الداخلي، وضغط الانكماس الناتج عن التدخل، والشكل الهندسي للأسطوانة. كما أن الأساليب التحليلية الكلاسيكية، بما في ذلك معادلات لامي ونظرية هرتز، غير كافية للتنبؤ الدقيق بإجهادات

التماس، والتشوهات اللدنية، والإجهادات المتبقية، عندما يصبح السلوك غير الخطى للمواد والتشوهات الكبيرة مؤثرين بشكل ملحوظ.

في هذه الدراسة، أُجري تحليل لاحظى باستخدام طريقة العناصر المتناهية باستخدام برنامج ABAQUS لدراسة ضغط التلامس، وتوزيع الإجهادات، والتشوه اللدن في أسطوانتين متحدتى المركز ومفتوحتى النهايتين من الألومنيوم والفولاذ، خاضعتين لظروف التركيب بالتدخل (Shrink-fit). في البداية، طُبق حمل أولى مقداره $66.5 \text{ ميجا نيون}/\text{م}^2$ ، ثم أزيل لاحقًا لتحقيق ضغط تداخل مستهدف قدره $1 \text{ ميجا نيون}/\text{م}^2$ عند السطح البيني بين الأسطوانتين بعد إزالة الحمل، ثم أعيد تطبيق نصف الحمل التمهيدى الأصلى ($33.25 \text{ ميجا نيون}/\text{م}^2$) لدراسة تطور الإجهادات، ونشوء الإجهادات المتبقية، وتفاعل المواد. بعد ذلك، قورنت النتائج المتحصل عليها بنتائج أسطوانة واحدة من الألومنيوم خاضعة لحمل مقداره $66.5 \text{ ميجا نيون}/\text{م}^2$. ظهر المقارنة أن التركيب بالتدخل يحسن توزيع الإجهادات ويقلل من القيم العظمى للإجهاد. وتتوفر هذه النتائج إطاراً منهجياً لتصميم تجمعات أسطوانية سميكة الجرمان تعتمد على التركيب بالتدخل، بما يتجاوز حدود الطرق التحليلية الكلاسيكية.

الكلمات المفتاحية: التداخل الحراري، الأسطوانات ذات الجرمان السميكة، المواد غير المتماثلة، الإجهادات المتبقية، التحليل غير الخطى بالعناصر المحددة.

Introduction

Shrink-fit assemblies are widely used in mechanical design to transmit torque and axial loads without auxiliary fasteners, with applications in cutting tool holders, wheels and bands for railway stock, gears, turbine discs, rotors for electric motors and for locating ball and roller bearings [1]. Traditionally, the mechanical behavior of these assemblies has been analyzed using elastic solutions derived from Lamé's theory for thick-walled cylinders [1,2]. These solutions provide analytical expressions for radial and hoop stresses under uniform interference but assume linear elasticity, small strains, and homogeneous materials, limiting their applicability to low interference levels and purely elastic conditions. Extensions using Hertzian contact theory have improved interface stress estimation [3], but such models remain restricted to elastic contact and idealised geometries.

Classical analytical models typically underestimate peak Cauchy stresses, failed to capture residual stress fields generated during unloading. These residual stresses are critical for structural integrity and fatigue performance, as compressive interface stresses can reduce tensile stress amplitudes and delay crack initiation [4]. However, excessive interference may induce plastic yielding in the softer component, causing stress redistribution, residual stress relaxation, and mechanical performance degradation [5]. Experimental and numerical studies have further highlighted that inappropriate preload selection can promote fretting damage and reduce fatigue life under cyclic loading [6].

Finite element analysis (FEA) has emerged as the primary tool for detailed shrink-fit analysis, overcoming limitations of classical solutions. Early linear elastic FEA models improved geometric flexibility but could not simulate elastoplastic behavior or residual stress development [7]. Nonlinear material models and surface-to-surface contact formulations have since enabled more realistic simulations [8]. Recent studies emphasize the importance of finite deformation kinematics, particularly for high interference materials. Neglecting large deformations leads to significant errors in predicted contact pressure, plastic strain accumulation, and residual stress distribution [9].

Preload optimization has been identified as a key design factor. Residual stress evolution depends strongly on interference magnitude, with an optimal range maximizing beneficial compressive stresses while limiting plastic deformation [10]. Fatigue strength is highly sensitive to these preload-induced stresses, especially in aluminum–steel assemblies under cyclic loading [11]. Despite these advances, gaps remain: most studies focus on compound shrink-fit assemblies without comparing them to equivalent single homogeneous cylinders, and few consider the complete stress evolution from assembly through service loading [12]. Recent advances in computational mechanics, together with the widespread availability of commercial finite element analysis (FEA) Softwares, have enabled comprehensive and design-oriented simulations of complex contact problems. Modern surface-to-surface contact formulations, finite-strain kinematics, and isotropic elastoplastic constitutive models, allow accurate prediction of contact pressure distributions, localized plastic deformation, and residual Cauchy stress fields following unloading [13].

The present study aims to perform a nonlinear finite element analysis of an aluminum–steel shrink-fit assembly, incorporating finite deformation kinematics and elastoplastic material behavior, to quantify residual stress development during assembly and its influence on stress redistribution under subsequent service loading. Additionally, the study compares the mechanical response of the compound shrink-fit configuration with that of an equivalent single homogeneous cylinder, assessing the design advantages and limitations of shrink-fit assemblies beyond the elastic regime.

2. Finite Element Model

2.1 Geometry and Material Properties

The assembly consists of two concentric, long, open-ended cylinders modeled using a two-dimensional axisymmetric representation. The inner cylinder is made of aluminum and represents the soft cylinder, while the outer cylinder is made of steel and represents the harder cylinder. This configuration captures the essential mechanical behavior of practical shrink fit joints while maintaining computational efficiency. A schematic of the assembly model is presented in Figure 1.

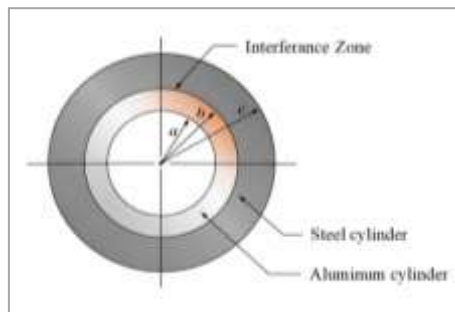


Figure 1: Schematic representation of the assembly model.

The material properties and geometric parameters used in the analysis are summarized in Table 1. Aluminum exhibits lower stiffness and yield strength, allowing plastic deformation to develop under high contact pressure, whereas steel remains predominantly elastic. The material hardening was modeled as isotropic.

Table 1 Material properties and geometric parameters

Material	E (GPa)	Poisson's Ratio (v)	ID (cm)	OD (cm)	Initial Yield (MPa)	Yield at 5000 μ m (MPa)
Aluminum	70	0.33	9.1	10.1	106	156
Steel	200	0.25	10.1	12.1	200	300

2.2 Contact Definition and Assembly

The two cylinders were assembled concentrically using the ABAQUS *Instance* module as shown in Figure 2. A small initial clearance was introduced to avoid numerical overlap prior to loading. Surface-to-surface contact was defined at the interface, with the inner surface of the steel cylinder designated as the master surface and the outer surface of the aluminum cylinder as the slave surface. This choice follows established contact modeling guidelines, ensuring numerical stability and minimizing mesh-induced penetration errors.

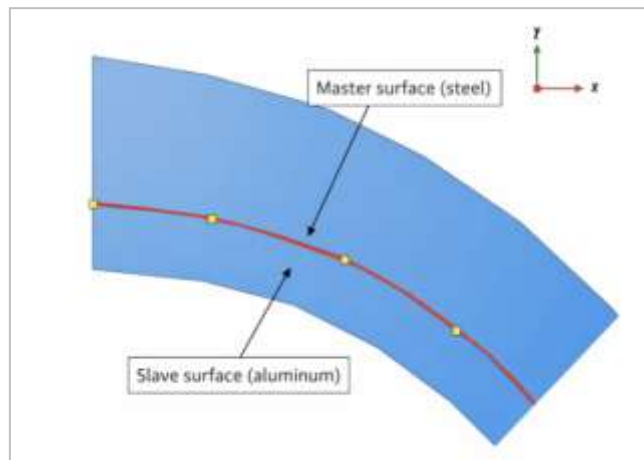


Figure 2: Shrink Fit Assembly

2.3 Boundary Conditions and Loading Procedure

Symmetry boundary conditions, as illustrated in Figure 3, were applied in both the axial and radial directions to prevent rigid body motion and ensure numerical stability. A controlled preload was applied as an internal pressure and iteratively adjusted to achieve a target residual interface pressure of 1 MN/m^2 after unloading. Through multiple iterations, an applied pressure of 66.5 MN/m^2 was determined to be sufficient to generate the desired residual interference pressure during the initial loading stage. This iterative approach ensures accurate development of residual stresses at the aluminum–steel interface, critical for the subsequent stress redistribution analysis.

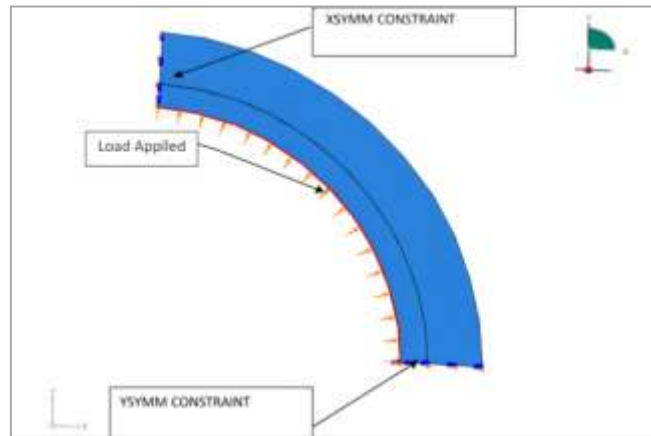


Figure 3: Boundary Conditions and Loads

2.4 Mesh Strategy and Element Type

A refined mesh, shown in Figure 4, was employed in the contact region using a biased meshing technique to accurately capture steep stress gradients at the interface. The slave surface (aluminum) was discretized with a finer mesh than the master surface (steel) to ensure accurate representation of localized plastic deformation. Four-node bilinear axisymmetric elements with reduced integration (CPE4R) were used under plane strain assumptions, appropriate for modeling long, open-ended cylinders. This meshing strategy ensures numerical stability while accurately resolving the elastoplastic behavior and contact pressure evolution at the interface.

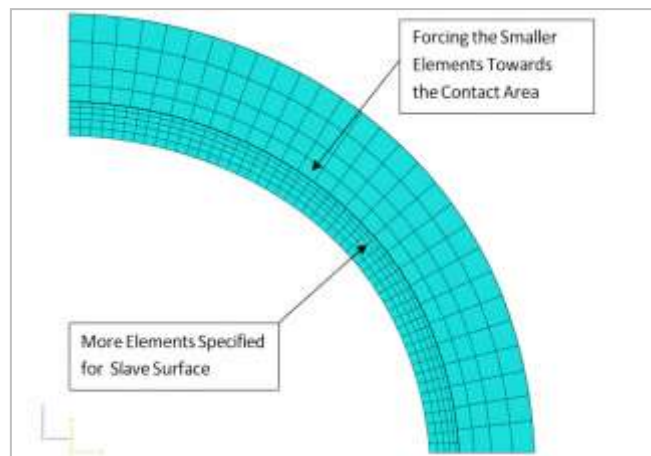


Figure 4: Meshing the Model

3. Results

The von Mises stress distribution shown in Figure 5, obtained after applying the initial interference pressure of 66.5 MN/m^2 , reveals an obvious stress concentration at the aluminum–steel interface. Stress magnitudes decrease radially inward within the aluminum and outward within the steel, reflecting the load transfer mechanisms and the difference in material stiffness. The localized high-stress regions correspond to plastic deformation zones, which are critical for the development of beneficial residual stresses. This stress pattern identifies critical regions

for fatigue assessment and demonstrates the capability of the nonlinear finite element model to accurately capture the realistic mechanical response of the compound shrink fit assembly.

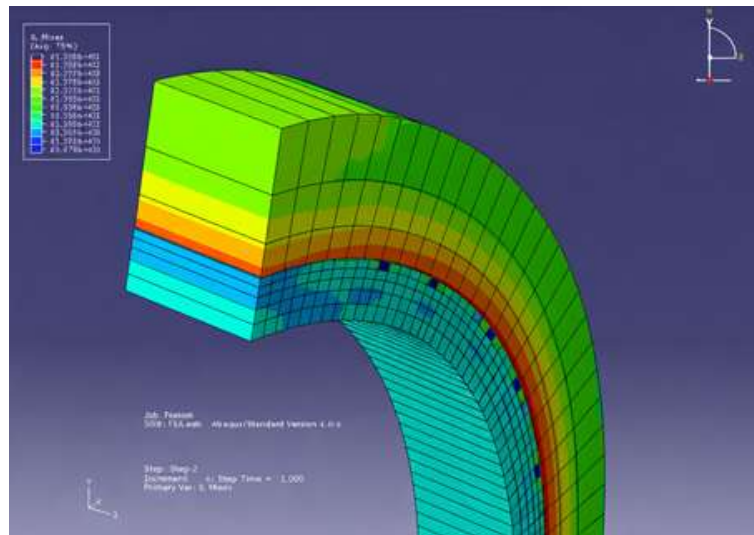


Figure 5: Von Mises stress distribution at the initial preload

Figure 6 illustrates the effect of residual stresses on the response of the joint under subsequent loading, showing the contact pressure distribution when half of the initial preload (33.25 MN/m^2) is reapplied. The interface stresses increase significantly compared with those generated by the applied pressure alone, reflecting the superposition of residual stresses from the previous preload. This emphasizes the importance of accounting for stress redistribution when evaluating service loads and highlights how pre-existing residual stress fields influence the overall joint behavior.

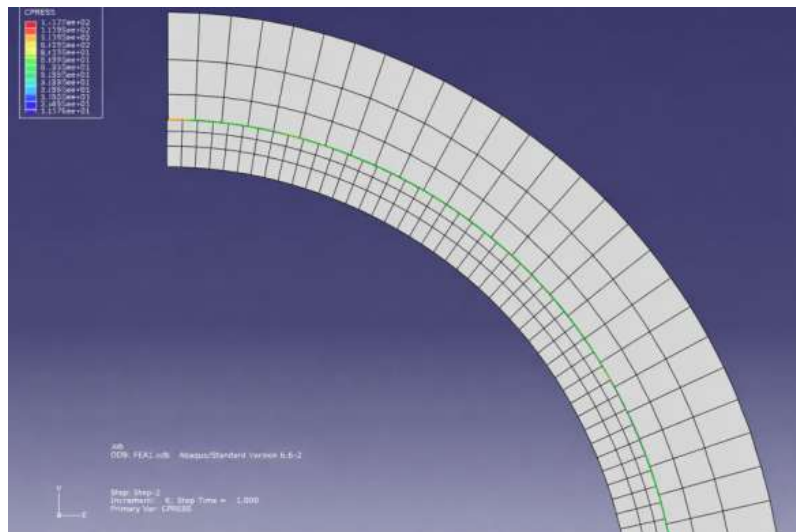


Figure 6: Maximum contact pressure at half of the initial preload

For comparison, Figure 7 shows the von Mises stress distribution in a single, homogeneous aluminum cylinder subjected to the same applied load of 66.5 MN/m^2 . Unlike the compound shrink fit configuration, the homogeneous cylinder exhibits a smooth stress gradient across the thickness, with maximum stresses concentrated at the inner radius and decreasing toward the outer surface. The absence of material interfaces prevents stress redistribution, resulting in higher localized stresses governed solely by geometry and bending effects. This comparison clearly demonstrates the advantage of the compound shrink fit design, where material interaction and residual stresses contribute to improved stress distribution, and reduced peak stress levels under identical loading conditions.

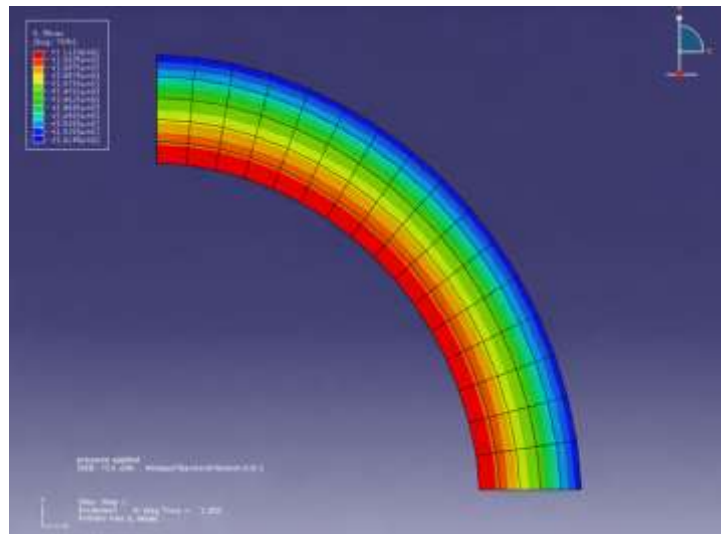


Figure 7: Von Mises stress in an aluminum cylinder

4. Discussion

Figure 8 illustrates the stress distributions along a radial path, extending from the inner bore of the aluminum cylinder to the outer surface of the steel cylinder.

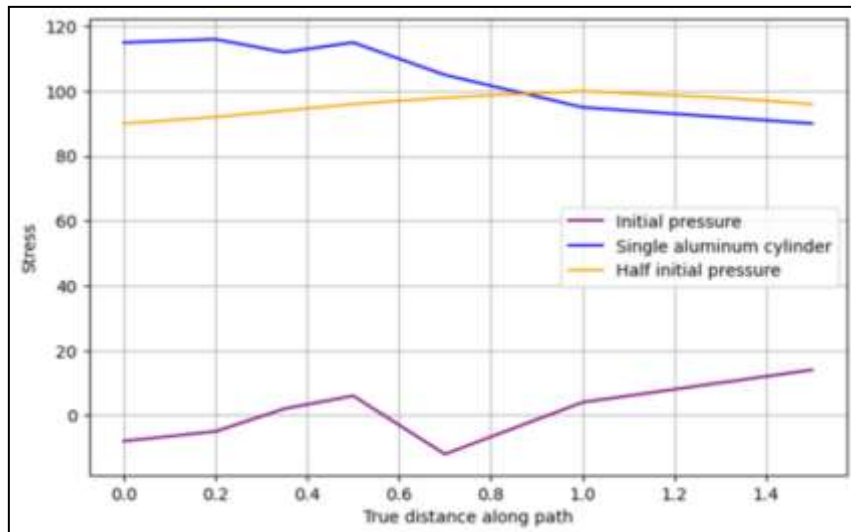


Figure 8: illustrates the stress distributions along a radial path.

Three cases are analyzed: the residual stress state induced by the interference preload (Initial pressure), the response of a single aluminum cylinder subjected to full internal pressure (Single aluminum cylinder), and the behavior of the assembled aluminum–steel system under a reduced load (Half initial pressure). For the Initial pressure case, an obvious stress peak is observed near the aluminum–steel interface, corresponding to the maximum contact pressure developed during assembly. Stress magnitudes decrease toward the inner bore, in agreement with classical compound cylinder theory. Nevertheless, deviations from the ideal elastic solution appear as localized stress fluctuations, which are attributed to material nonlinearity and localized plastic deformation within the aluminum cylinder caused by the shrink fit.

In the Single aluminum cylinder case, the stress reaches its maximum at the inner surface and decreases nonlinearly toward the outer radius, as expected. This case exhibits the highest peak stress, reflecting that the aluminum cylinder alone must sustain the full applied pressure. The Half initial pressure case demonstrates substantially lower stress levels while retaining a similar overall distribution, indicating a predominantly linear elastic response. Comparison across the three cases highlights the load-sharing contribution of the steel cylinder, which reduces stresses in the aluminum cylinder and introduces beneficial compressive residual stresses, thereby improving the structural performance of the assembly.

5. Conclusions

This study has demonstrated the effectiveness of nonlinear finite element analysis in predicting contact stresses, plastic deformation, and residual stress development in aluminum–steel shrink fit assemblies. Controlled preload application generates beneficial compressive residual stresses that significantly reduce peak contact stresses and improve load sharing between cylinders. Conversely, excessive preload leads to localized plastic deformation and non-uniform stress distributions that may compromise fatigue performance.

The findings highlight the critical role of preload magnitude and material compliance mismatch in shrink fit design. Integrating optimized preload strategies with nonlinear finite element modeling provides a robust framework for enhancing the durability, reliability, and fatigue resistance of shrink fit and press fit joints in engineering applications.

Future Work

Based on the findings of this study, the authors recommend the following areas for future research:

- A more detailed investigation into the influence of friction between mating surfaces should be conducted to better understand its impact on interference behavior and stress distribution.
- Future studies should incorporate full three-dimensional finite element models to capture more realistic geometries and loading conditions, as the current analysis is limited to axisymmetric models.
- The fatigue life of shrink-fit assemblies under cyclic loading should be analyzed through numerical simulation to evaluate long-term performance and identify potential failure mechanisms.

Compliance with ethical standards

Disclosure of conflict of interest

The authors declare that they have no conflict of interest.

References

- [1] J. D. Booker, C. E. Truman, S. Wittig, and Z. Mohammed, “A comparison of shrink-fit holding torque using probabilistic, micromechanical and experimental approaches,” *Proc. Inst. Mech. Eng., Part B: J. Eng. Manuf.*, vol. 218, no. 2, pp. 175–187, 2004.
- [2] S. Choudhury, *Stress Analysis of Thick Walled Cylinder*, Ph.D. dissertation, 2013.
- [3] G. Fu, “An extension of Hertz’s theory in contact mechanics,” *J. Appl. Mech.*, vol. 74, no. 2, pp. 373–374, 2007, doi: 10.1115/1.2188017.
- [4] A. Özel, S. Temiz, M. D. Aydin, and S. Sen, “Stress analysis of shrink fitted joints for various fit forms via finite element method,” *Mater. Des.*, vol. 26, pp. 281–289, 2005, doi: 10.1016/j.matdes.2004.06.014.
- [5] N. Laghzale and A. Bouzid, “Analytical modelling of elastic-plastic interference fit joints,” *Int. Rev. Model. Simul.*, vol. 9, no. 3, pp. 191–199, 2016.
- [6] J. Juoksukangas, A. Lehtovaara, and A. Mäntylä, “Experimental and numerical investigation of fretting fatigue behavior in bolted joints,” *Tribol. Int.*, vol. 103, pp. 440–448, 2016.
- [7] R. S. Falk, “Finite element methods for linear elasticity,” in *Mixed Finite Elements, Compatibility Conditions, and Applications*, Berlin, Germany: Springer, 2008, pp. 159–194.
- [8] T. Pore, S. G. Thorat, and A. A. Nema, “Review of contact modelling in nonlinear finite element analysis,” *Mater. Today: Proc.*, vol. 47, pp. 2436–2440, 2021.
- [9] Y. Wang, S. Xiang, and H. Zhang, “Multi-constraint assembly error modeling and optimization method for centrifugal compressors considering manufacturing errors and assembly deformation,” *Measurement*, Art. no. 120094, 2025.
- [10] R. Su, L. Huang, C. Xu, P. He, X. Wang, B. Yang, and H. Ma, “Factors influencing residual stresses in cold expansion and their effects on fatigue life—A review,” *Coatings*, vol. 13, no. 12, Art. no. 2037, 2023.
- [11] C. Zhang, R. Sun, J. Yin, Y. Hu, Q. Dou, Z. Tang, and Y. Li, “Failure behaviours of steel/aluminium threaded connections under impact fatigue,” *Eng. Fail. Anal.*, vol. 174, Art. no. 109473, 2025.
- [12] C. Wang, M. Du, M. Zheng, and Q. Sun, “Study on the stress evolution at threads of bolted joint under transverse loads,” *Proc. Inst. Mech. Eng., Part C: J. Mech. Eng. Sci.*, vol. 239, no. 6, pp. 2106–2116, 2025.
- [13] R. Jackson, I. Chusoipin, and I. Green, “A finite element study of the residual stress and deformation in hemispherical contacts,” *J. Tribol.*, vol. 127, no. 3, pp. 484–493, 2005.

Disclaimer/Publisher’s Note: The statements, opinions, and data contained in all publications are solely those of the individual author(s) and contributor(s) and not of **AJAPAS** and/or the editor(s). **AJAPAS** and/or the editor(s) disclaim responsibility for any injury to people or property resulting from any ideas, methods, instructions, or products referred to in the content.